Anja Heyse, Matthias Kraume, Anja Drews

The impact of lipases on the rheological behavior of colloidal silica nanoparticle stabilized Pickering emulsions for biocatalytical applications

Heyse, A., Kraume, M., & Drews, A. (2020). The impact of lipases on the rheological behavior of colloidal silica nanoparticle stabilized Pickering emulsions for biocatalytical applications. Colloids and Surfaces B: Biointerfaces, 185, 110580. https://doi.org/10.1016/j.colsurfb.2019.110580

The impact of lipases on the rheological behavior of colloidal silica nanoparticle stabilized Pickering emulsions for biocatalytical applications

Anja Heyse[a,c,*], Matthias Kraume[b], Anja Drews[a]

[a] HTW Berlin – University of Applied Sciences, Engineering II, Life Science Engineering, Wilhelminenhofstraße 75A, 12459 Berlin, Germany
[b] TU Berlin, Chair of Chemical and Process Engineering, Straße des 17. Juni 135, 10623 Berlin, Germany
[c] TU Berlin, Chair of Food Technology and Food Material Science, Königin-Luise-Str. 22, 14195 Berlin, Germany

Anja Heyse, anja.heyse@campus.tu-berlin.de

Matthias Kraume, matthias.kraume@tu-berlin.de

Anja Drews, anja.drews@htw-berlin.de

*Corresponding author: Anja Heyse

Technische Universität Berlin

Königin-Luise-Str. 22, 14196 Berlin, Germany

Tel.: 0049-3031471797; Fax: 0049-3031471492

eMail: anja.heyse@campus.tu-berlin.de

ABSTRACT (max. 200 words)

The use of Pickering emulsions for biocatalytical applications has recently received increased attention in cases where hydrophobic reactants are involved. For process applications, knowledge of the emulsion's rheology is crucial for the fluid dynamical design of equipment and selection of operating conditions. Colloidal silica nanoparticle stabilized Pickering emulsions usually exhibit shear-thinning behavior caused by a complex particle-particle network. While this has been observed by many authors, no publication has yet dealt with the rheology of silica nanoparticle stabilized Pickering emulsions containing enzymes. Thus, the aim of this study was to investigate the impact of the commonly used biocatalyst lipase (type and concentration), the dispersed phase volume fraction and the silica particle concentration on the rheological behavior of water-in-oil Pickering emulsions. For this purpose, the impact of the named parameters on the viscosity curves were measured. Lipases reduced the viscosities and transferred the rheological behavior from shear-thinning to Newtonian, which might be due to interactions of the lipase molecules via the formation of intermolecular disulfide bonds, which disturb the hydrogen-bond based silica particle-particle network. However, by increasing the dispersed phase volume fraction or the silica particle concentration the rheological behavior of emulsions became again shear-thinning. This work will help to produce bioactive Pickering emulsions with tailor-made characteristics.

GRAPHICAL ABSTRACT

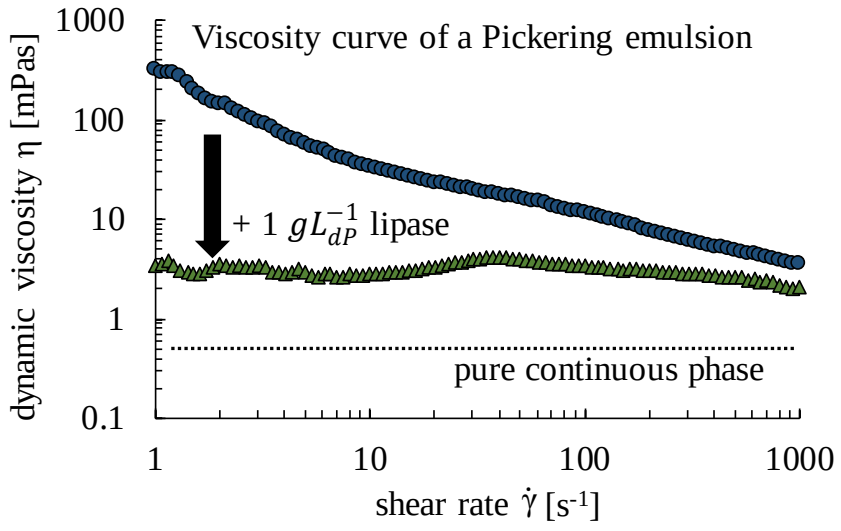

KEY WORDS

Rheology, shear-thinning, lipase, Pickering emulsions, colloidal silica nanoparticles

ABBREVIATIONS

CalA	*Candida antarctica* lipase A
CalB	*Candida antarctica* lipase B
cP	continuous phase
CPME	cyclopentyl methyl ether
dP	dispersed phase
LipTL	Lipase TL from *Pseudomonas stutzeri*
NE	no enzyme
PE	Pickering emulsion
w/o	water-in-oil

SYMBOLS

c_i	[gL^{-1}]	concentration of compound i
$d_{D,i}$	[µm]	droplet diameter
$d_{1,0}$	[µm]	arithmetic mean diameter
$d_{3,2}$	[µm]	Sauter mean diameter
N_D	[-]	number of droplets
V_{dP}	[L]	volume of dispersed phase
V_{cP}	[L]	volume of continuous phase
$\dot{\gamma}$	[s^{-1}]	shear rate
η	[mPa s]	dynamic viscosity
φ_{dp}	[-]	dispersed phase volume fraction

1. INTRODUCTION

To cover the high demand of synthesis involving hydrophobic substrates and/or products, biocatalysis in unconventional media (*i.e.*, organic solvents) is a powerful technique leading to high yields [1–3]. However, biocatalysts require a minimum water activity in the media to achieve an adequate catalytic activity [4–6]. To provide this, two-phase systems in which the biocatalyst is located in the aqueous phase, guaranteeing its activity, and the hydrophobic reactants predominate in the organic phase are promising alternatives. During the reaction, the

reactants will come into contact with the biocatalyst at the interface; hence, a high interfacial area is needed for high reaction rates. To that end, high power must be introduced to the system (*i.e.*, by stirring [5, 7]), which might damage the biocatalysts due to shear stress can [8].

Lipases are interfacially active enzymes of special interest for the biotechnological production of fine chemicals and pharmaceutically active compounds [9–11] that are easily deactivated by shearing [8, 12]. In this context, the application of nanoparticle-stabilized emulsions, so-called Pickering emulsions (PEs) appears to be a promising option to create stable dispersed droplets with large interfacial areas and a minimal energy input [13, 14]. The feasibility of using water-in-oil (w/o) PEs for biocatalysis has been proven to positively affect their activity [13]. Even without stirring the PE, higher yields were achieved for lipase-catalyzed reactions in w/o PEs in batch processes in comparison to batch reactions in stirred dispersions [15]. Furthermore, continuous lipase-catalyzed reactions with a subsequent liquid-liquid separation have been recently demonstrated in a fixed-bed reactor or a membrane reactor [14, 16]. Particularly in the case of continuous operations, the fluid dynamical design of equipment and operating conditions, *e.g.*, for the latter case membrane modules, the rheological behavior and flow properties of an emulsion are significant characteristics. PEs can be stabilized by colloidal silica nanoparticles, which easily adsorb at interfaces [3, 16–18] and which can create a thixotropic and shear-thinning rheological behavior [19]. This is due to a particle-particle network formed by hydrogen bonds between residual silanol groups on the surface of the silica nanoparticles. This network is highly affected by interfacially active additives, such as proteins, and can be interrupted and destabilized [20]. Furthermore, the shear-thinning character of an emulsion is more pronounced for fine and monodisperse than for coarse and polydisperse emulsions [21]. It can be expected that the rheological properties of PEs are influenced by interfacially active lipases due to their ability to adsorb to interfaces [22, 23] and due to their impact on reducing the droplet sizes and on increasing the monodispersity of w/o PEs [16, 24]. However, no literature about the rheology of PEs containing lipases is available yet. To that end, the impact of lipases on the rheological behavior of w/o PEs was investigated in this study. Colloidal silica nanoparticles were used to prepare the w/o PEs and the impact of the lipase type, dispersed phase volume fraction, silica nanoparticle concentration and lipase concentration on the viscosity curves and the drop size distributions of the PEs was evaluated.

2. MATERIALS AND METHODS

2.1. Materials

Cyclopentyl methyl ether (CPME) (8465.360, VWR, Germany) was used as the continuous phase since it had already been used for lipase-catalyzed reactions in previous studies [16, 24].

The lipases *Candida antarctica* lipase A (CalA), Lipase TL from *Pseudomonas stutzeri* (LipTL), and *Candida antarctica* lipase B (CalB) were purified by dialysis with a 10 mM phosphate buffer (dialysis tube with 14 kDa molecular weight cut off, D9527, Sigma Aldrich Chemie GmbH, Germany) and lyophilized. The dialyzed and lyophilized lipase powder (16-17 % total protein content determined with Bradford assay) were kindly provided by the research group of M.B. Ansorge-Schumacher (Technische Universität Dresden, Germany). The properties and structural characteristics of the used lipases are listed in Table 1. Casein sodium salt was purchased from Sigma Aldrich Chemie GmbH, Germany (C8654-500G). The colloidal silica nanoparticles HDK® H20 used in this study were kindly donated by Wacker Chemie, Germany. For all experiments, ultra-pure water was used.

Table 1: Properties and structural characteristics of the used lipases CalA, CalB, and LipTL.

	CalA [25]	CalB [25]	LipTL [26]
molecular weight [kDa]	45 [27]	33 [28]	27
isoelectric point	7.5	6	6.6
pH optimum	7	7	7-8
thermostability [°C]	<70	<60 [29]	<40
pH stability	6-9	7-10	6-9
protein conformation	globular	globular	globular
presence of typical lipase lid	yes	no (α-helix instead)	yes
interfacial activation	yes	no	yes
number of intramolecular disulfide bonds	2 [30]	3 [31]	3 [32]

2.2. Pickering emulsion preparation

Silica nanoparticles were dispersed in the continuous phase (cP) CPME. Ultrapure water was used as a dispersed phase (dP) to minimize salts effects from the buffer [33, 34]. The lipase (LipTL, CalA or CalB) was dissolved in the aqueous dispersed phase (dP). The phases were dispersed using a rotor/stator homogenizer (UltraTurrax T25, IKA GmbH, Germany) at 17500 min^{-1} for two minutes.

The dispersed phase volume fraction was varied from 0.1-0.5 and is defined as:

$$\varphi_{dP} = \frac{V_{dP}}{V_{cP+}V_{dP}} \quad (1)$$

A w/o PE with a dispersed volume fraction of 0.7 was unstable. The silica nanoparticle and lipase concentration were varied between 15-60 gL_{dP}^{-1} and 1-5 gL_{dP}^{-1} (regarding the dispersed phase), respectively. The specific parameters used for the investigation in this study are listed in Table 2.

Table 2: Parameters used for emulsion preparation

Emulsion composition	Varied parameters for the specific investigations on the rheological behavior of a w/o PE			
	impact of lipase type	impact of dispersed phase volume fraction	impact of silica nanoparticle concentration	impact of lipase concentration
lipase type	LipTL, CalA, CalB	CalA	CalA	CalA
φ_{dP} [-]	0.2	0.1, 0.2, 0.5	0.2	0.2
$c_{particle}$ [gL_{dP}^{-1}]	15	15	15, 30, 40, 50, 60	60
c_{lipase} [gL_{dP}^{-1}]	1	1	1	1, 3, 5

2.3. Image acquisition and drop size determination

Microscopic pictures (Axio Scope A1 Microscope, Zeiss, Germany) of PE samples were taken with a magnification factor of 20. Emulsion samples were diluted 10-fold with the continuous phase to visualize separate droplets. SOPAT image analysis software (Smart Online Particle Analysis Technology – SOPAT GmbH, Berlin, Germany) was used for data evaluation, picture analysis and droplet size measurement [35, 36].

The Sauter mean diameter ($d_{3,2}$) (eq. (2)) and the arithmetic mean diameter ($d_{1,0}$) (eq. (3)) were calculated from the droplet diameters $d_{D,i}$ of at least N_D = 500 droplets of each sample.

$$d_{3,2} = \sum_{i=1}^{n} d_{D,i}^3 / \sum_{i=1}^{n} d_{D,i}^2 \quad (2)$$

$$d_{1,0} = \sum_{i=1}^{n} \frac{d_{D,i}}{N_D} \quad (3)$$

The ratio of arithmetic to Sauter mean diameter (eq. (4)) is used as an indicator of the degree of monodispersity of the PE: the larger the ratio, the greater is the monodispersity.

$$degree_{monodisp} = \frac{d_{1,0}}{d_{3,2}} \quad (4)$$

2.4. Rheological measurement

An MCR 302 rheometer (Anton Paar GmbH, Germany) was used to measure the rheological behavior. The term rheological behavior is used in this study to describe the group of fluid classifications determined by shear rheology. From previous experiments, the emulsion

droplet sizes were expected to be up to 50 µm [16]. To ensure a gap size of at least 10-fold larger than the expected droplet sizes, a plate and plate measurement system (PP50; 49.97 mm diameter) with a gap size of 0.5 mm was used for all experiments. All emulsions were shaken before measurements to avoid droplet sedimentation. Shaking does not affect the droplet size distribution of w/o PE stabilized with colloidal silica nanoparticles [37]. The rheological behavior (fluid classification) was analyzed using shear rates from 1 to 1000 s^{-1} (logarithmic ramp) to ensure comparability with the relevant literature [17, 18, 38, 39]. Afterwards, the same sample was also analyzed from 1000 to 1 s^{-1} to study potential hysteresis effects. Rheology measurements were performed at 20.0 ± 0.1 °C. All experiments were performed in triplicate.

3. RESULTS AND DISCUSSION

3.1. Impact of lipase type

The viscosity curves of w/o PEs containing no enzymes (NE-PE) or one of the three lipases (LipTL-, CalA-, and CalB-PE) are shown in Fig 1A. The NE- and CalB-PE showed shear-thinning behavior (indicated by a decreasing curve), while the LipTL- and CalA-PE showed Newtonian flow behavior (indicated by a horizontal curve).

The HDK® H20 stabilized NE-PE possessed shear-thinning behavior, which indicates the presence of attractive forces of the particles between the emulsion droplets. These attractive forces caused the formation of a weak, elastic network via hydrogen bonds of the residual silanol groups on the particle surface [19]. A highly pronounced shear-thinning behavior was also observed for 1-dodecene based w/o PEs prepared with the same silica nanoparticles HDK® H20 (no bioadditives), which was explained by the strong ability of HDK® H20 to form networks in the nonpolar solvent [18]. The viscosities of the w/o PEs prepared with either 1-dodecene [18] or CPME (this study) were comparable, even though the viscosity of pure 1- dodecene (1.3 mPas [18]) is about twice the viscosity of pure CPME (0.55±0.05 mPas, own triplicate measurements) at the same temperature, and 1-dodecene is more hydrophobic ($logP_{1\text{-dodecene}}$ = 6.8 vs. $logP_{CPME}$ = 1.3 [40, 41]). Raghavan *et al.* found that the residual silanol groups of the particles interact directly and build hydrogen bonds with adjacent particles and not with the weakly hydrogen bonding solvent [42]. Hence, the viscosities and rheological behavior of w/o PEs are predominated by the used particles and the formed particle-particle network rather than the used organic solvents.

The addition of the lipases CalA and LipTL transformed the rheological behavior of the PE from shear-thinning to Newtonian (Fig. 1A). In contrast, for shear rates lower than 100 s^{-1}, the CalB-PE showed shear-thinning behavior comparable to the NE-PE. Despite CalB-PE showing shear-thinning behavior, its viscosity was comparable to the viscosities of the CalA- and LipTL-PEs for shear rates >100 s^{-1}. A small bump indicating shear-thickening behavior of PE can be observed around 30, 6, and 2 s^{-1} for CalA-, LipTL- and CalB-PE, respectively. Bumps were also found for w/o PEs without bioadditives, in which the increasing appearance of bumps was related to decreasing shear-thinning behavior of the w/o PEs [18]. The shear-thinning behavior of emulsions is a result of weak particle-particle interactions (hydrogen bonds). The switch of the rheological behavior of emulsions from shear-thinning behavior to Newtonian behavior can be caused by an interruption of the built particle-particle network, *i.e.*, due to electric repulsion caused by small changes of the pH [20]. Lipases at the interface of water-oil systems reduce the interfacial tension causing a 'skin' formation due to intermolecular disulfide bonds, which has been described during the aging at interfaces [22]. Hence, the lipases may also interrupt the hydrogen bonds based particle-particle network causing the observed bumps and transition of the rheological behavior. However, the amount of disulfide bonds differs based on the type of lipase [22]. The difference in the surface structures of the lipases used in this study is due to their mechanisms for the protection against denaturation of the enzyme at liquid-liquid interfaces (see table 1). CalA and LipTL have a typical lipase lid structure that protects the active center and leads to the interfacial activation of the enzyme (both are interfacially active lipases); whereas CalB possesses an α-helix molecular structure covering the active center. Due to those molecular differences, CalB might have formed fewer disulfide bonds than CalA and LipTL, which would explain why the stiffening of the emulsion network might be less pronounced in the CalA- or LipTL-PE than in the CalB-PE. Therefore, the CalB-PE showed only a slight reduction of the viscosity in comparison to NE-PE and still showed a shear-thinning behavior caused by the HDK® H20 particle-particle network.

The Sauter mean diameter of the investigated PEs, as well as the ratio of the arithmetic mean diameter to the Sauter mean diameter ($d_{1,0}/d_{3,2}$) (an indicator of the monodispersity of an emulsion) are depicted in Fig.1B. Here, all lipases significantly decreased the Sauter mean diameter of the w/o PE and showed a higher degree of monodispersity (*i.e.*, ratio of $d_{1,0}/d_{3,2}$) when compared to NE-PE. Among the lipase-PEs, CalB-PE had the largest Sauter mean diameter, and LipTL-PE the smallest. In a previous study about the filterability of lipase containing PEs stabilized with spherical silica particles, a decrease of the Sauter mean diameter was also observed when CalA or LipTL were added, but not for CalB [24]. The used lipases

varied in their molecular size and structure. The sizes of LipTL, CalA, and CalB were 27, 45 and 33 kDa, respectively [25, 26, 28]. Almost all lipases possess a hydrophilic protein structure lid [43], which protects the hydrophobic active center located inside the protein, and that opens and exposes the active center when lipase is adsorbed at the interface. Thus, the hydrophobic active center sticks out to the organic phase [44]. This activation mechanism is the same for almost all lipases. In comparison to CalA and LipTL, CalB has a helix structure instead of the typical lipase lid structure and does not exhibit an interfacial activation behavior [45]. Hence, the differences in the molecular size and structure of the lipases might cause the observed differences in the droplet size of the lipase-PEs.

For the rheological behavior of w/o PE, it can be concluded that all used lipases decreased the viscosity and decreased the shear-thinning behavior. The impact of the lipases was more pronounced for CalA and LipTL than for CalB. Furthermore, the addition of the lipases possessing the typical lipase lid structure, namely CalA and LipTL, resulted in the transfer of the rheological behavior of the w/o PE from shear-thinning to Newtonian rheological behavior. In biocatalytical batch reactions, the lipase CalA showed the highest activity in w/o PE (Supplementary information, Fig. S2); thus, CalA was chosen for further investigations.

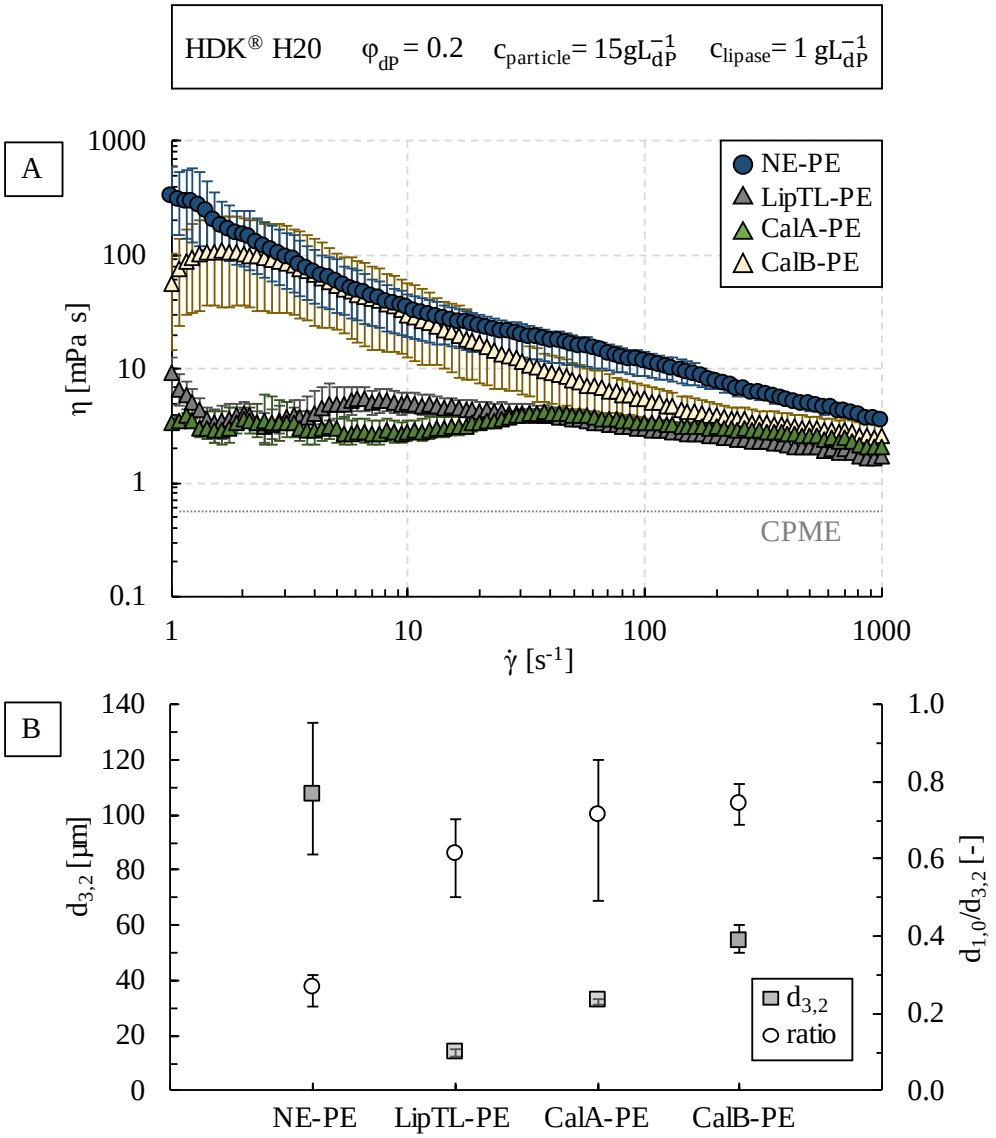

Fig.1: A) Emulsion viscosity (at 20 °C) as a function of shear rate and B) Sauter mean diameter $d_{3,2}$ and ratio of arithmetic to Sauter mean diameter ($d_{1,0}/d_{3,2}$) for w/o PEs without enzyme (NE) or containing 1 gL_{dP}^{-1} lipase (CalA, CalB, or LipTL). PEs were stabilized with 15 gL_{dP}^{-1} HDK® H20 colloidal silica nanoparticles and the dispersed phase volume fraction was 0.2. The hysteresis of the viscosity curve of HDK® H20 stabilized PE was negligible, thus, for clarity reasons, only the viscosity curves for 1 to 1000 s^{-1} were depicted. The dotted grey line represents the viscosity of the continuous phase CPME. Measurements were performed in triplicates. Error bars represent max. and min. error.

3.2. Impact of dispersed phase volume fraction

The viscosity curves of CalA-PEs prepared with several dispersed phase volume fractions (0.1-0.5) are shown in Fig 2A. The viscosity and the degree of shear-thinning behavior of a CalA-PE increase with increasing dispersed phase volume fraction. The viscosity of the emulsion with a dispersed phase volume fraction of 0.2 was slightly higher than that of the emulsion with a dispersed phase volume fraction of 0.1 (at shear rates above 10 s^{-1}), but both

emulsions showed Newtonian flow behavior (Fig. 2A). At smaller shear rates (<10 s^{-1}), the CalA-PE prepared with a 0.1 dispersed phase volume fraction showed a bump in the viscosity curve. As discussed before, the appearance of a bump is related to the beginning of shear-thickening behavior. In contrast, the emulsion with a dispersed phase volume fraction of 0.5 showed shear-thinning behavior. This might be due to that fact that the increase in dispersed phase volume led to more dispersed phase droplets per emulsion volume. Hence, droplets are closer to each other and particle-particle network bonding between colloidal silica nanoparticles (hydrogen bonds) is more likely to occur, which also creates emulsions being more stable against coalescence [38]. However, for the PE without CalA (NE-PE) but with the silica particle concentration and dispersed phase volume fraction, the NE-PEs demonstrated shear-thinning behavior without any differences in viscosity curves (see Fig. S1A, Supplementary information).

The Sauter mean diameter of the CalA-PE slightly decreased with increasing dispersed phase volume fraction (Fig. 2B). However, the degree of monodispersity of the CalA-PEs varied strongly. This is in contrast to the results obtained for NE-PEs, where the Sauter mean diameter increased with increasing dispersed phase, while the degree of monodispersity stayed constant (see Fig. S1B, Supplementary information). The latter was also observed for 1-dodecene based w/o PEs (no bioactive additives) [18]. Hence, the observed impact of the dispersed phase volume fraction of the CalA-PEs on the rheological behavior cannot be related to the droplet sizes. Another aspect can be the amount of stabilizing particles. Here, the amount of stabilizing particles per volume of the dispersed phase was kept constant. By that, it was ensured that observed effects are not caused by the relatively decreased availability of particles and the Sauter mean diameter was indeed almost unaffected (see Fig. 2B). For CalA-PE, the increase of dispersed phase volume fraction might increase the probability of droplets coming close into contact, and thus it might increase the silica particle-particle interaction. Thus, it can be concluded that the increase in dispersed phase volume fraction due to an increase of particle-particle interaction outweighed the impact of the lipase on the rheological behavior.

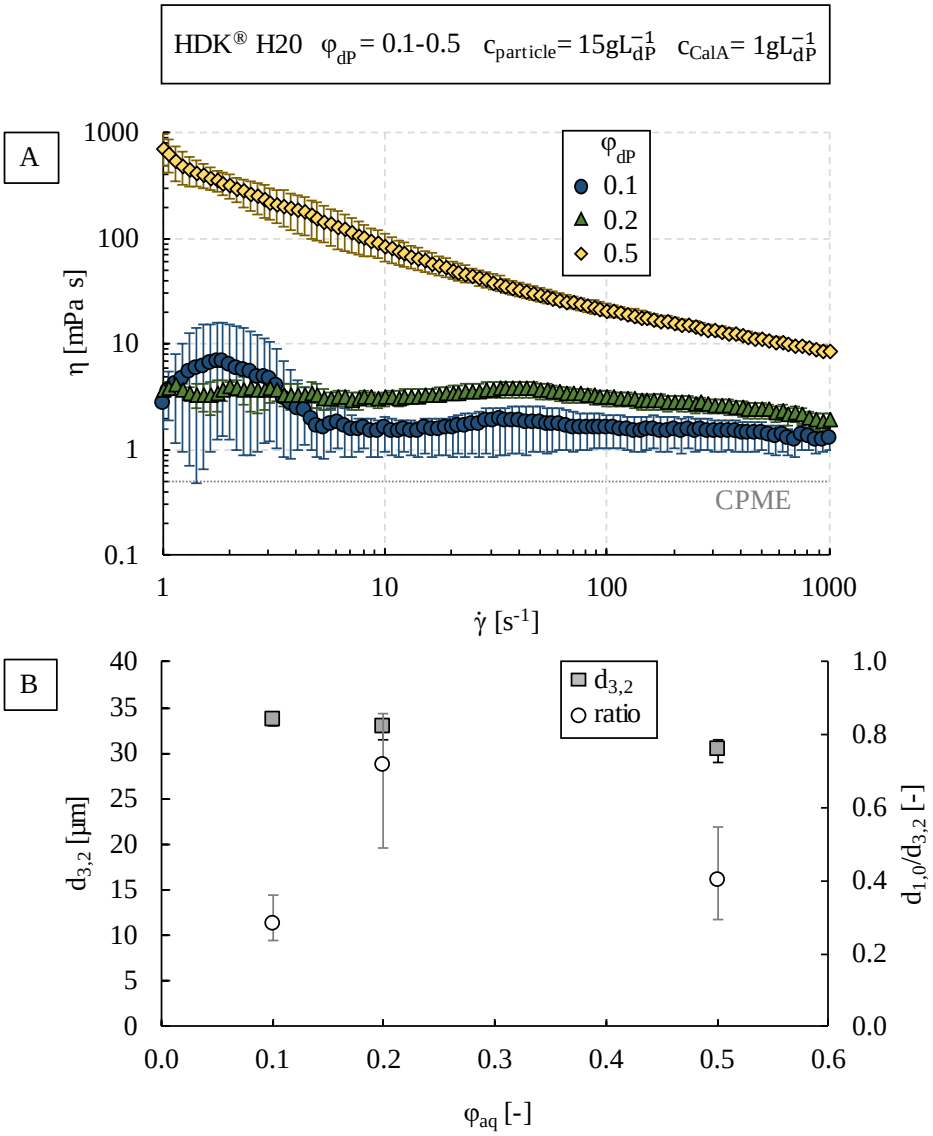

Fig 2: A) Emulsion viscosity (at 20 °C) as a function of shear rate and B) Sauter mean diameter $d_{3,2}$ and ratio of arithmetic to Sauter mean diameter ($d_{1,0}/d_{3,2}$) for w/o PEs containing 1 gL_{dP}^{-1} CalA-PEs were stabilized with 15 gL_{dP}^{-1} HDK® H20 colloidal silica nanoparticles and the dispersed phase volume fraction was varied from 0.1 to 0.5.

3.3. Impact of colloidal silica nanoparticle concentration

The viscosity curves of CalA-PEs prepared with several concentrations of the colloidal silica nanoparticles (15-60 gL_{dP}^{-1}) are shown in Fig 3A. The shear-thinning behavior of a CalA-PE increased with increasing silica nanoparticle concentration. The CalA-PE prepared with < 30 gL_{dP}^{-1} HDK® H20 showed almost Newtonian flow behavior while at higher concentrations they presented shear-thinning behavior. In all cases, at 1000 s^{-1}, the viscosities of the CalA-PEs did not vary anymore due to the high applied shear stress, which broke the particle-particle network of the PE regardless of the amount of used particles. In contrast to the 15 gL_{dP}^{-1}

HDK® H20 stabilized CalA-PE, all other CalA-PE do not show a bump around 30 s^{-1}. The viscosity of CalA-PE stabilized with 15 gL_{dP}^{-1} HDK® H20 decreased by the factor of 2 from 4 to 2 mPas with increasing shear rate. In contrast, the viscosities of CalA-PE stabilized with 60 gL_{dP}^{-1} HDK® H20 decreased by a factor of 75 from 150 to 2 mPas with increasing shear rate. The CalA-PE prepared with 60 gL_{dP}^{-1} HDK® H20 had the same rheological behavior as the NE-PE prepared with 15 gL_{dP}^{-1} HDK® H20 (compare to Fig. 1A).

The Sauter mean diameter of the CalA-PE decreased with increasing HDK® H20 concentration (see Fig. 3B) because the additional particles helped to stabilize smaller droplets with a larger total interfacial area [18]. The degree of monodispersity of the CalA-PE (ratio of $d_{1,0}/d_{3,2}$) varied only slightly and no significant differences could be observed for the HDK® H20 stabilized CalA-PE. The deviation of the Sauter mean diameter was relatively small (± 2.6 µm). Hence, the deviation of the ratio (+0.15/-0.2) was mainly due to the deviation of the arithmetic mean diameter (± 7µm).

For the rheological behavior of w/o PE, it can be concluded that the increase of the silica particle concentration outweighed the impact of the lipase. This can be due to the fact that with increasing silica nanoparticle concentration, the amount of excess silica that was not bound in the emulsion interface increased [46]. This excess silica can form and create a particle-particle network between single droplets in the continuous phase. This might explain why with increasing silica nanoparticle concentration in the dP; the rheological behavior of the PE was mostly defined by the HDK® H20 particles (shear-thinning flow behavior) rather than by the lipase. The particle-particle interaction outweighed the effect of the lipase in the same way as it was observed for increasing dispersed phase volume fraction. A scheme of possible PE properties at low and high silica particle concentration with or without the presence of lipases is given in Fig. 4.

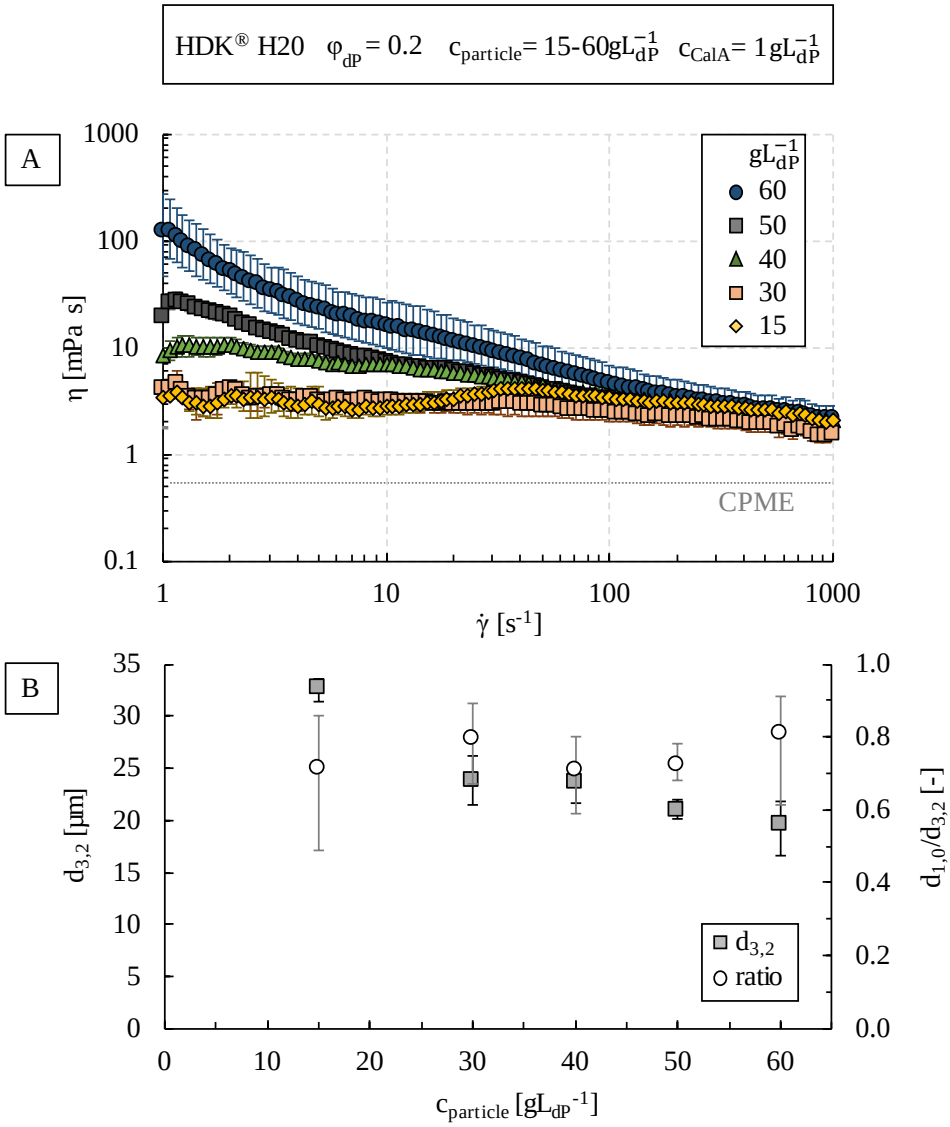

Fig. 3: A) Emulsion viscosity (at 20 °C) as a function of shear rate and B) Sauter mean diameter $d_{3,2}$ and ratio of arithmetic to Sauter mean diameter ($d_{1,0}/d_{3,2}$) for w/o PEs without enzyme (NE) or containing 1 gL_{dP}^{-1} CalA. PEs were stabilized with 15 gL_{dP}^{-1} HDK® H20 colloidal silica nanoparticles.

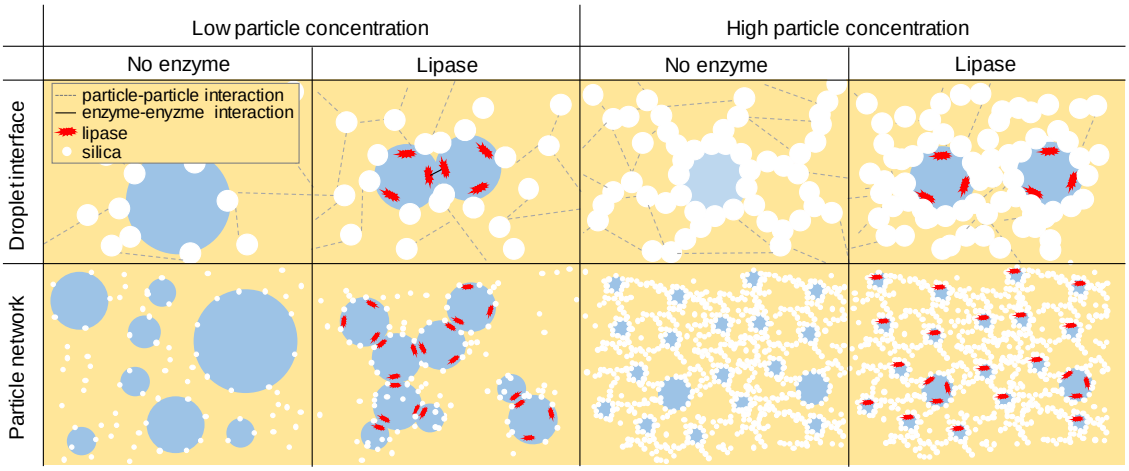

Fig. 4: Hypothetical scheme of w/o PE properties at low and high silica particle concentrations with or without the presence of lipases. Lipases are embedded in the sublayer. Dashed lines represent silica particle-particle interaction (hydrogen bonds). Solid lines illustrate disulfide bonds caused by enzyme-enzyme interactions of two lipases. Adapted from [24].

3.4. Impact of lipase concentration

The viscosity curves of CalA-PEs prepared with several lipase concentrations (1-5 gL_{dP}^{-1}) are shown in Fig 5A. The viscosity curves of the CalA-PEs remained constant for all evaluated concentrations of lipase. Here, a silica particle concentration of 60 gL_{dP}^{-1} was used, at which the impact of the lipase was already outweighed (see Fig. 3A). Hence, the impact of outweighing was also present when the concentration of lipase was increased. The ratio of lipase to silica concentration of 1 gL_{dP}^{-1} to 15 gL_{dP}^{-1} (~0.07, Newtonian; see data from chapter 3.1) was within the range of used ratios in this chapter, namely 3 to 60 (~0.05, shear-thinning) and 5 to 60 (0.08, shear-thinning), but showed different rheological behavior. Hence, the lipases, which are embedded in an interfacial sublayer, might only disturb the particle-particle network due to formation of intermolecular disulfide bonds between lipase molecules until a specific surface coverage degree by the silica particles is reached. This competition for the available spaces will also influence the reaction rates and yields through both its influence on droplet size and thus available mass transfer area and also on the number of biocatalyst molecules at the reaction site.

The Sauter mean diameter decreased by about 60 % from 19.61 +2.16/-2.91 µm to 7.32 +1.10/-0.72 µm with increasing lipase concentration from 1 to 5 gL_{dP}^{-1} (see Fig. 5B). However, the degree of monodispersity (<0.8) remained constant with increasing lipase concentration. The adsorption kinetics of lipase and silica nanoparticles differ significantly. Even though silica nanoparticles stabilize the emulsion interface, they do not reduce the interfacial tension [47]. In contrast, lipase significantly reduces the interfacial tension: the

interfacial tension (after 500 s) of a vegetable oil/ water system (without any further surfactants) was reduced about 26 % by adding lipase [48], while it was only reduced about 2 % by adding silica nanoparticles [47]. The addition of interfacial active substances reduces the interfacial tension, which causes the decrease of the droplet size and enhances the resistance against coalescence [49]. Hence, the increase of lipase concentration might lead to more embedded lipases in the sublayer which might further decrease the interfacial tension. This would explain the observed decrease of the droplet size of lipase containing Pickering emulsions.

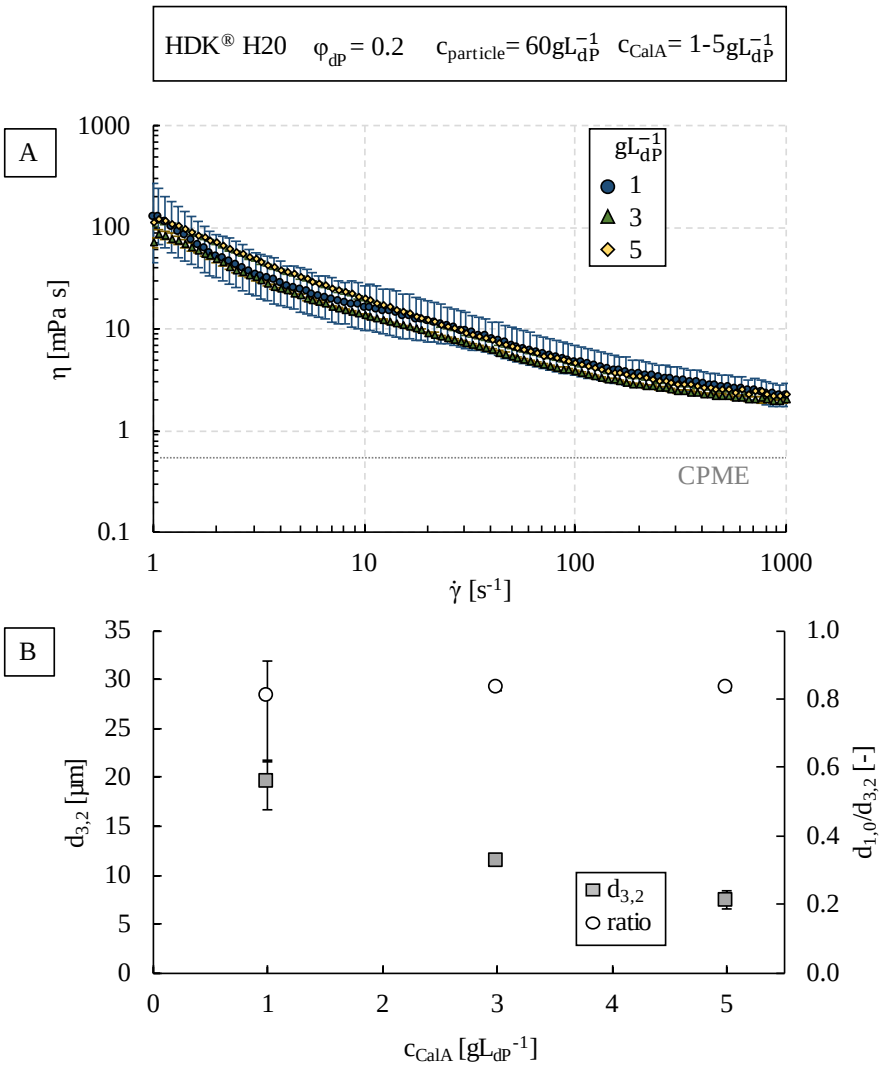

Fig. 5: A) Emulsion viscosity (at 20 °C) as a function of shear rate and B) Sauter mean diameter $d_{3,2}$ and ratio of arithmetic to Sauter mean diameter ($d_{1,0}/d_{3,2}$) for w/o PEs containing 1-5 gL_{dP}^{-1} CalA. PEs were stabilized with 60 gL_{dP}^{-1} HDK® H20 colloidal silica nanoparticles.

4. CONCLUSIONS

In order to study the impact of the biocatalyst on the rheological properties of a nanoparticle-stabilized two-phase system, the impact of the lipase type, the dispersed phase volume fraction, the colloidal silica nanoparticle concentration and the lipase concentration of water-in-oil Pickering emulsions stabilized with colloidal silica nanoparticles was investigated.

It was shown that the addition of the lipases (Lipase TL from *Pseudomonas stutzeri*, *Candida antarctica* lipase A or B) reduced of the viscosity and the shear-thinning behavior. Furthermore, when the lipases possessed the typical lipase lid structure, the rheological behavior was transferred from shear-thinning to Newtonian rheological behavior. In addition, the lipases significantly reduced the droplet size of the Pickering emulsion. The differences in rheological behavior and drop sizes might be caused by different molecular properties of the lipases. With higher dispersed phase volume fraction or silica nanoparticle concentration, the effects of the lipases on the rheological behavior of the Pickering emulsion was outweighed, by the higher degree of particle-particle interaction. In contrast, the increase of lipases concentration had no effect on the rheological behavior of the Pickering emulsion but further decreased the droplet size.

In combination with the obtained results, it can be concluded that the impact of the lipases is relevant until the interface is fully covered by the silica particles and/or for dilute emulsions (low dispersed phase volume fractions). Lipase is still quite small in comparison to the interfacial pore size between colloidal silica at the interface and thus, even if the interface is fully covered, the lipase can still act at those pores. However, the high interface coverage by particles diminishes the number of biocatalyst molecules that can reach the reaction site. In addition, H20 have been found to form multilayers which decrease the overall mass transfer rate at excessive particle concentrations [50]. The drop size of colloidal silica nanoparticle stabilized water-in-oil Pickering emulsions depends on the used lipase source and can be tuned by varying the concentration of the particles and/or the concentration of lipases. In turn, this affects the viscosity and rheological behavior of lipase containing Pickering emulsions, which are crucial parameters for the design of operating conditions or process equipment: *e.g.*, for the design of a membrane reactor for the continuous liquid/liquid separation of the emulsion.

ACKNOWLEDGMENT

Financial support of the project BioPICK (031A163A) by the German Federal Ministry for Education and Research (BMBF) is greatly acknowledged. The authors thank the group of Prof. M.B. Ansorge-Schumacher (Technische Universität Dresden) and Wacker Chemie GmbH for providing enzymes and silica particles. Anja Heyse thanks Melanie Kaiser and Minh Chau Luong Boi for the supporting work, as well as Markus Kolano and Dr. Rocio Morales Medina for discussion.

REFERENCES

[1] S.S. Kaki, P. Adlercreutz, Chem. Phys. Lipids. 164 (2011) 246–250.

[2] J. Mangas-Sánchez, M. Serrano-Arnaldos, P. Adlercreutz, J. Mol. Catal. B Enzym. 112 (2014) 9–14.

[3] T. Skale, D. Stehl, L. Hohl, M. Kraume, R. von Klitzing, A. Drews, Chem. Ing. Tech. 88 (2016) 1827–1832.

[4] S. Damodaran, Water at Biological Phase Boundaries: Its Role in Interfacial Activation of Enzymes and Metabolic Pathways, in: Disalvo E. Membr. Hydration. Subcell. Biochem., Springer International Publishing, 2015: pp. 233–261.

[5] A. Zaks, A.M. Klibanov, J. Biol. Chem. 263 (1988) 8017–8021.

[6] L. Ma, M. Persson, P. Adlercreutz, Enzyme Microb. Technol. 31 (2002) 1024–1029.

[7] W. Chulalaksananukul, FEBS Lett. 276 (1990) 181–184.

[8] S.E. Charm, B.L. Wong, Biotechnol. Bioeng. 12 (1970) 1103–1109.

[9] K.-E. Jaeger, T. Eggert, Curr. Opin. Biotechnol. 13 (2002) 390–397.

[10] Z. Amini, Z. Ilham, H.C. Ong, H. Mazaheri, W.H. Chen, Energy Convers. Manag. 141 (2017) 339–353.

[11] R.D. Schmid, R. Verger, Analysis. 37 (1998) 1608–1633.

[12] Y. Lee, C. Choo, Biotechnol. Bioeng. 33 (1989) 183–190.

[13] C. Wu, S. Bai, M.B. Ansorge-Schumacher, D. Wang, Adv. Mater. 23 (2011) 5694–5699.

[14] M. Zhang, L. Wei, H. Chen, Z. Du, B.P. Binks, H. Yang, J. Am. Chem. Soc. 138 (2016) 10173–10183.

[15] L. Wei, M. Zhang, X. Zhang, H. Xin, H. Yang, ACS Sustain. Chem. Eng. 4 (2016) 6838–6843.

[16] A. Heyse, C. Plikat, M. Ansorge-Schumacher, A. Drews, Catal. Today. 331 (2019) 60–

67.

[17] H. Katepalli, V.T. John, A. Tripathi, A. Bose, J. Colloid Interf. Sci. 485 (2017) 11–17.

[18] L. Hohl, S. Röhl, D. Stehl, R. von Klitzing, M. Kraume, Chem. Ing. Tech. 88 (2016) 1815–1826.

[19] G. Wacker Chemie AG, Product overview 6180de/05.10 - “HDK - Pyrogene Kieselsäure,” 2010.

[20] J.S. Weston, J.H. Harwell, B.P. Grady, Soft Matter. 13 (2017) 6743–6755.

[21] R. Pal, AIChE J. 42 (1996) 3181–3190.

[22] P. Reis, R. Miller, J. Kra, M. Leser, V.B. Fainerman, H. Watzke, K. Holmberg, Langmuir. 24 (2008) 6812–6819.

[23] A. Sarkar, S. Zhang, M. Holmes, R. Ettelaie, Adv. Colloid Interfac. 263 (2019) 195–211.

[24] A. Heyse, C. Plikat, M. Gruen, S. Delaval, M. Ansorge-Schumacher, A. Drews, Process Biochem. 72 (2018) 86–95.

[25] O. Kirk, M.W. Christensen, Org. Process Res. Dev. 6 (2002) 446–451.

[26] L. Meito Sangyo Co., Product specifications Lipase TL from Pseudomonas stutzeri, Triacylglycerol lipase EC 3.1.1.3, Nikko-cho, Japan, 2017.

[27] D.D. Kitts, Trends Food Sci. Technol. 16 (2005) 549–554.

[28] P. Nicolás, V.L. Lassalle, M.L. Ferreira, Enzyme Microb. Technol. 97 (2017) 97–103.

[29] C. Jun, B.W. Jeon, J.C. Joo, Q.A.T. Le, S.-A. Gu, S. Byun, D.H. Cho, D. Kim, B.-I. Sang, Y.H. Kim, Process Biochem. 48 (2013) 1181–1187.

[30] ‘Uniprot Protein Database-CalA’. [Online]. Available: https://www.uniprot.org/uniprot/W3VKA4. [Accessed: 01-Oct-2019].

[31] ‘Uniprot Protein Database-CalB’. [Online]. Available: https://www.uniprot.org/uniprot/P41365. [Accessed: 01-Oct-2019].

[32] ‘Uniprot Protein Database-LipTL’. [Online]. Available: https://www.uniprot.org/uniprot/O59952. [Accessed: 01-Oct-2019].

[33] B.P. Binks, R. Murakami, S.P. Armes, S. Fujii, Langmuir. 22 (2006) 2050–2057.

[34] F. Yang, S. Liu, J. Xu, Q. Lan, F. Wei, D. Sun, J. Colloid Interf. Sci. 302 (2006) 159–169.

[35] S. Maaß, J. Rojahn, R. Hänsch, M. Kraume, Comput. Chem. Eng. 45 (2012) 27–37.

[36] R.P. Panckow, G. Comandè, S. Maaß, M. Kraume, Chem. Eng. Technol. 38 (2015) 2011–2016.

[37] D. Stehl, L. Hohl, M. Schmidt, J. Hübner, M. Lehmann, M. Kraume, R. Schomäcker, R. von Klitzing, Chem. Ing. Tech. 88 (2016) 1806–1814.

[38] A. Pajouhandeh, A. Kavousi, M. Schaffie, M. Ranjbar, Colloids Surf. A. 520 (2017) 597–611.

[39] N. Kumar, T. Gaur, A. Mandal, J. Ind. Eng. Chem. 54 (2017) 304–315.

[40] ‘PubChem Database - 1-dodecene (CID 8183)’. [Online]. Available: https://pubchemdocs.ncbi.nlm.nih.gov. [Accessed: 11-Sep-2018].

[41] ‘PubChem Database - CPME (CID 138539)’. [Online]. Available: https://pubchem.ncbi.nlm.nih.gov. [Accessed: 11-Sep-2018].

[42] S.R. Raghavan, H.J. Walls, S.A. Khan, Langmuir. 16 (2000) 7920–7930.

[43] K. Saulich, Reaktionskinetische Experimente zur Lipase-katalysierten Hydrolyse von Rapsöl in Wasser-in-Öl-Emulsionen, 2008. http://opus.kobv.de/btu/volltexte/2009/597/.

[44] Z.S. Derewenda, A.M. Sharp, Trends Biochem. Sci. 18 (1993) 20–25.

[45] D.J. Ericsson, A. Kasrayan, P. Johansson, T. Bergfors, A.G. Sandström, J.-E. Bäckvall, S.L. Mowbray, J. Mol. Biol. 376 (2008) 109–119.

[46] J. Frelichowska, M.A. Bolzinger, Y. Chevalier, J. Colloid Interf. Sci. 351 (2010) 348–356.

[47] R. Pichot, F. Spyropoulos, I.T. Norton, J. Colloid Interf. Sci. 377 (2012) 396–405.

[48] C.J.J. Beverung, C.J.J. Radke, H.W.W.U. Blanch, Biophys. Chem. 81 (1999) 59–80.

[49] S. Tcholakova, N.D. Denkov, T. Banner, Langmuir. 20 (2004) 7444–7458.

[50] M. Petzold, S. Röhl, L. Hohl, D. Stehl, M. Lehmann, R. von Klitzing, M. Kraume, Chem. Ing. Tech. 89 (2017) 1561–1573.

SUPPORTING MATERIAL (SUPPLEMENTARY INFORMATION)

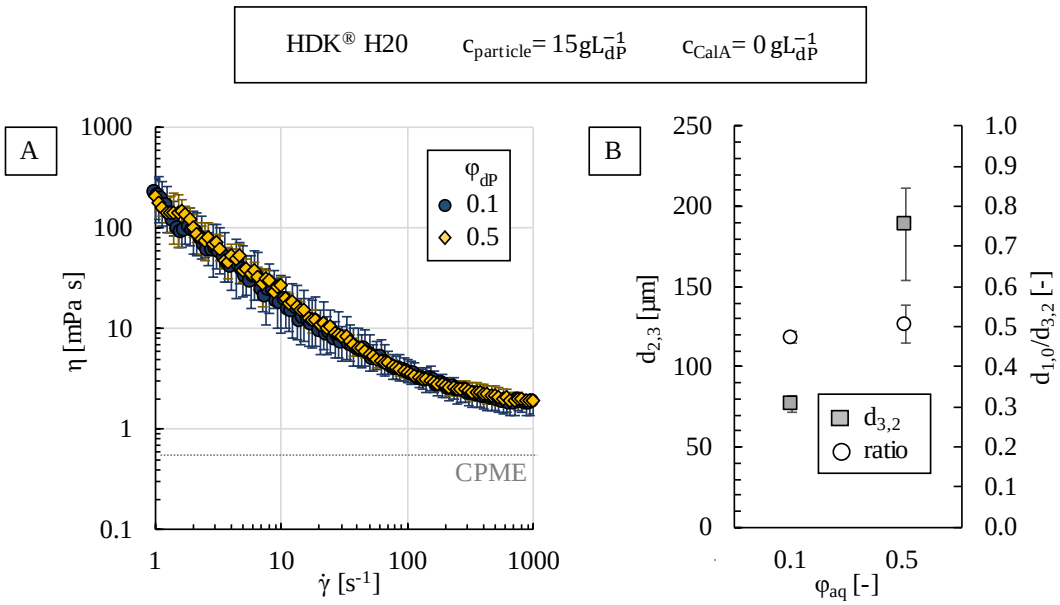

Fig. S1: A) Emulsion viscosity (at 20 °C) as a function of shear rate and B) Sauter mean diameter $d_{3,2}$ and the ratio of arithmetic to Sauter mean diameter ($d_{1,0}/d_{3,2}$) for w/o NE-PEs stabilized with 15 gL_{dP}^{-1} HDK® H20 colloidal silica nanoparticles. The dispersed phase volume fraction was either 0.1 or 0.5.

Batch reactions with different types of lipases

The lipase-catalyzed transesterification of 1-phenyl ethanol with vinyl butyrate to 1-phenylethyl butyrate was chosen as a model reaction, which has already been used in previous studies (biocatalysis in w/o PEs) [16, 24].

The transesterification was performed by using a total emulsion volume of 20 mL with an aqueous volume fraction of 0.2. The dP contained 1 gL_{dP}^{-1} lipase (CalA, CalB, or LipTL) in 50 $mmolL^{-1}$ phosphate buffer pH 7. The continuous phase was CPME. The emulsion was prepared as described in *Materials and Methods*. The PE was stirred at 500 min^{-1} and the temperature was set to 35 °C. To start the reaction (batch-wise mode), the substrate 1-phenyl ethanol (82 $mmolL^{-1}$) and the co-substrate vinyl butyrate (520 $mmolL^{-1}$) was added to the emulsion. The co-substrate concentration was chosen to be 6 times higher, so that co-substrate limitation can safely be neglected. The sample which was taken from the emulsions was centrifuged for 10 min at 14000 g to separate the liquids. Product (1-phenylethyl butyrate) concentration in the continuous phase was analyzed by HPLC (Knauer GmbH, Germany) on a C18 phase column (Machery Nagel, EC 125/4 Nucleosil 100 5) with 60 % ethanol in MilliQ water as the eluent. 100 µL of the continuous phase of the separated emulsion was mixed with

900 µL EtOH and analyzed. The flow rate and temperature were set to 0.5 $mLmin^{-1}$ and 25 °C, respectively. The samples were analyzed with a UV detector (K-2600, Knauer GmbH, Germany) at 254 nm wavelength.

Fig. S2 shows the time-dependent product concentration for the transesterification catalyzed by the three lipases. The highest product formation was observed for CalA-PE, while the product formation was significantly lower for LipTL- and CalB-PE. The substrate range of the lipases are different; thus, the chosen model reaction might be feasible for CalA, but not for LipTL or CalB.

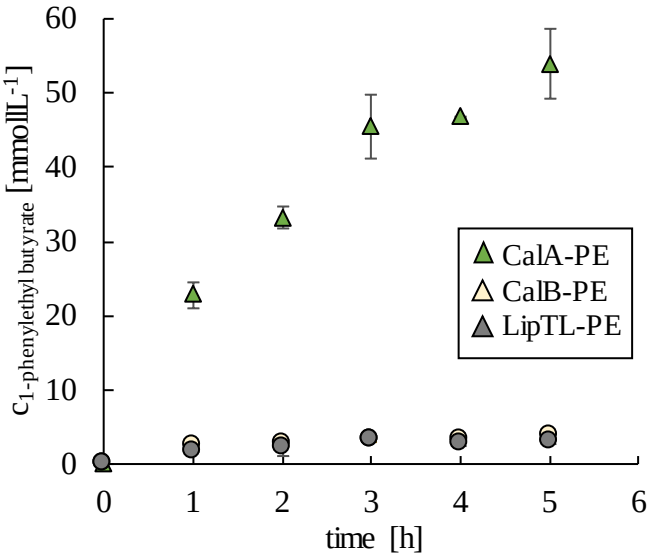

Fig. S2: Product concentration over time for transesterification catalyzed with lipases in w/o PEs ($c_{particle}$=30 gL_{dP}^{-1}; φ_{aq}=0.2; dP: 1 gL_{dP}^{-1} lipase in 50 $mmolL^{-1}$ phosphate buffer pH 7.2. Measurements represent technical triplicates. Error bars represent max. and min. error.